Supporting Information-

Rich-Phosphorus/Nitrogen Co-doping Carbon Boosting the Kinetics of Potassium-ion Hybrid Capacitors

Zhenyu Xie[†], Jiannian Xia [†,‡], Daping Qiu[†], Jinying Wei[†,‡], Min Li[†], Feng Wang[†,§,], Ru Yang[†,‡,]**

[†] *State Key Laboratory of Chemical Resource Engineering, Beijing Key Laboratory of Electrochemical Process and Technology for Materials, Beijing University of Chemical Technology, Beijing 100029, P. R. China.*

[‡] *Changzhou Institute of Advanced Materials, Beijing University of Chemical Technology, Changzhou, Jiangsu 213000, P. R.China.*

[§] *Beijing Advanced Innovation Center for Soft Matter Science and Engineering, Beijing University of Chemical Technology, Beijing 100029, P. R.China.*

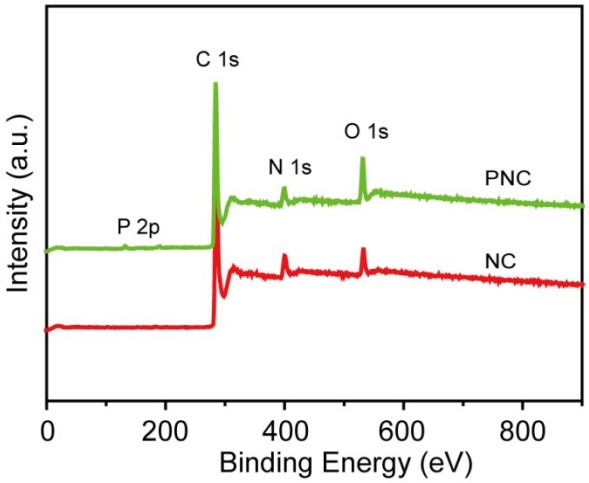

Figure S1. XPS spectra of NC and PNC

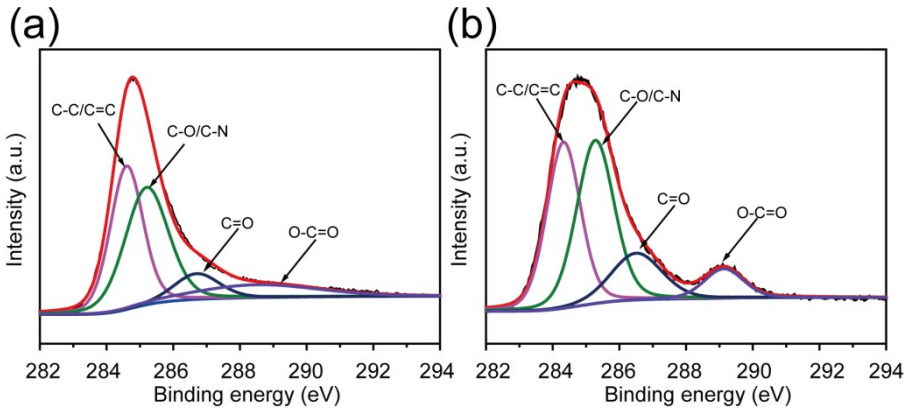

Figure S2. C1s XPS spectra of (a) NC and (b) PNC

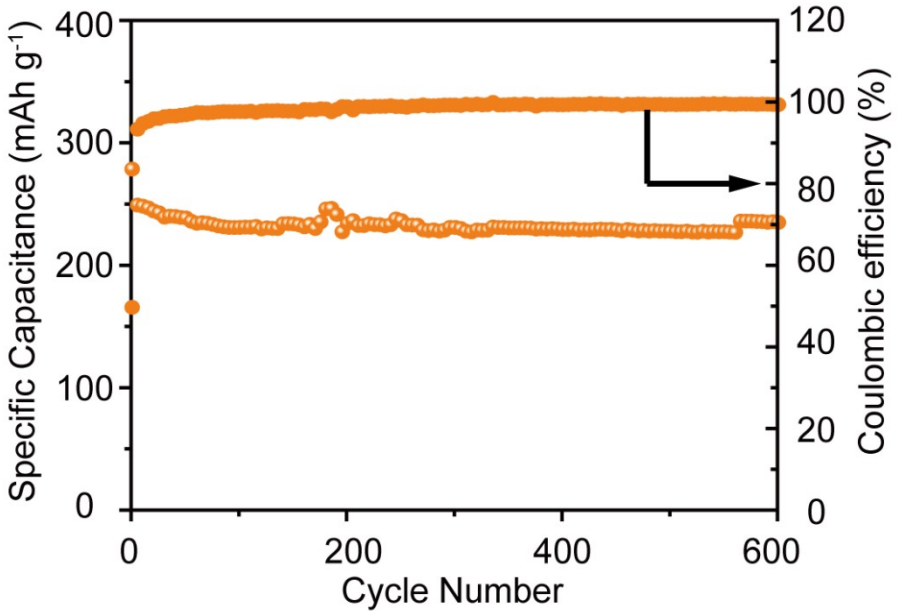

Figure S3. Long cycling performance of PNC at 0.2 A g^{-1}

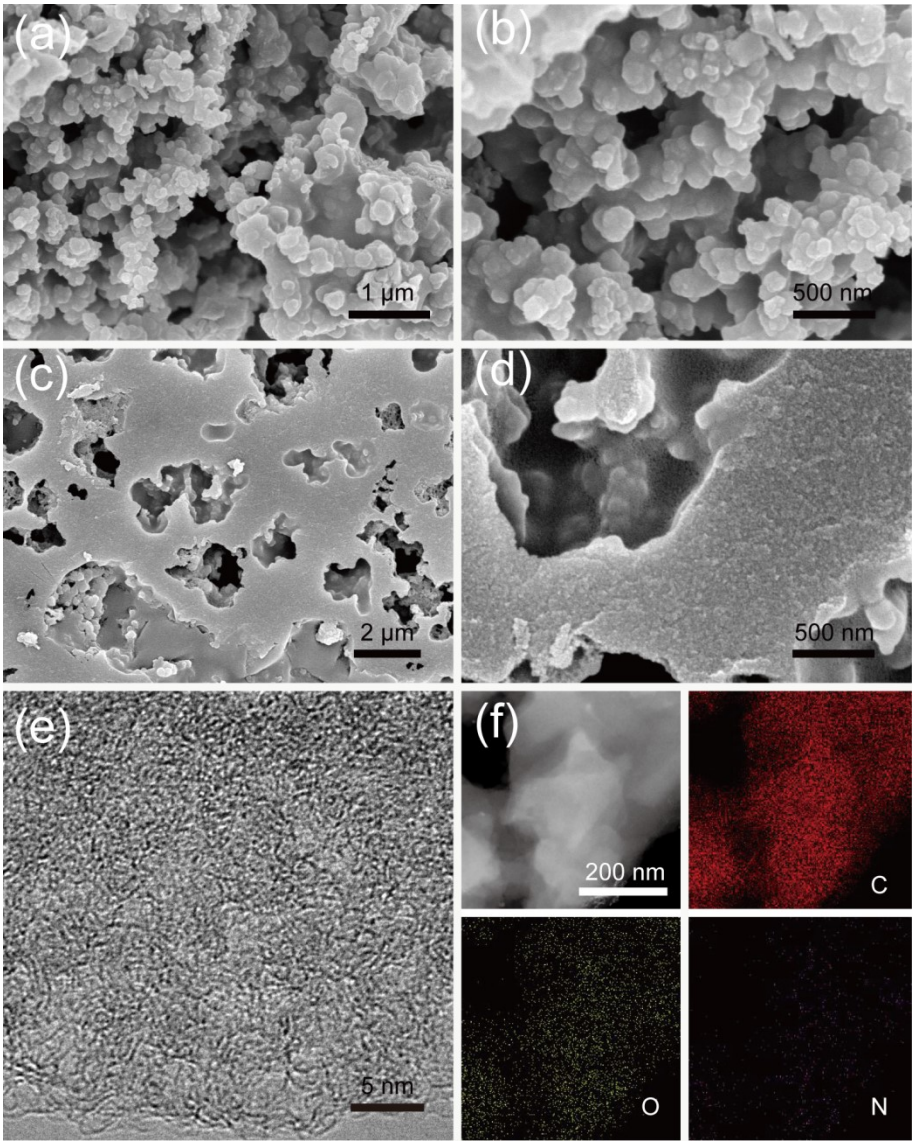

Figure S4. (a), (b) SEM images of precursors. (c), (d) SEM images, (e) HRTEM image and (d) Mapping images of HPC

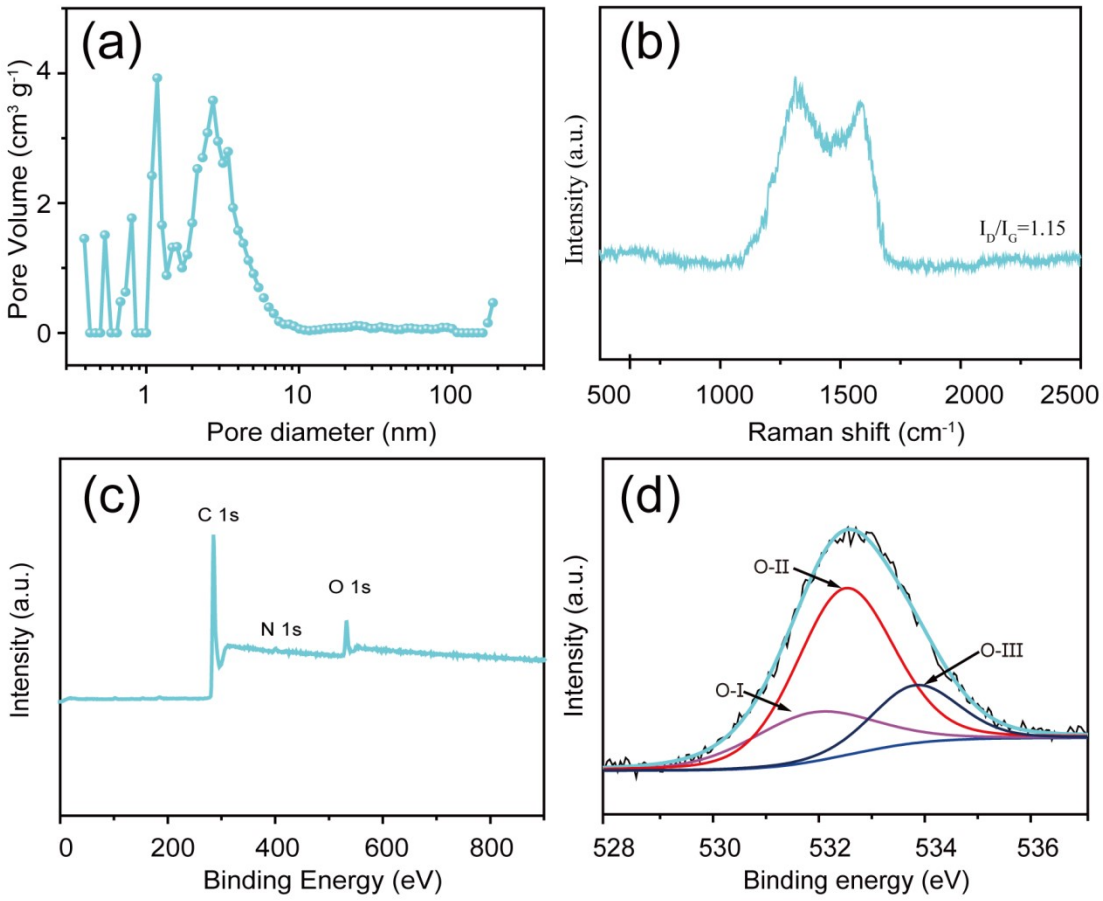

Figure S5. (a) pore size distributions of HPC, (b) Raman spectrum, (c) XPS spectrum and O 1s high-resolution spectrum of HPC

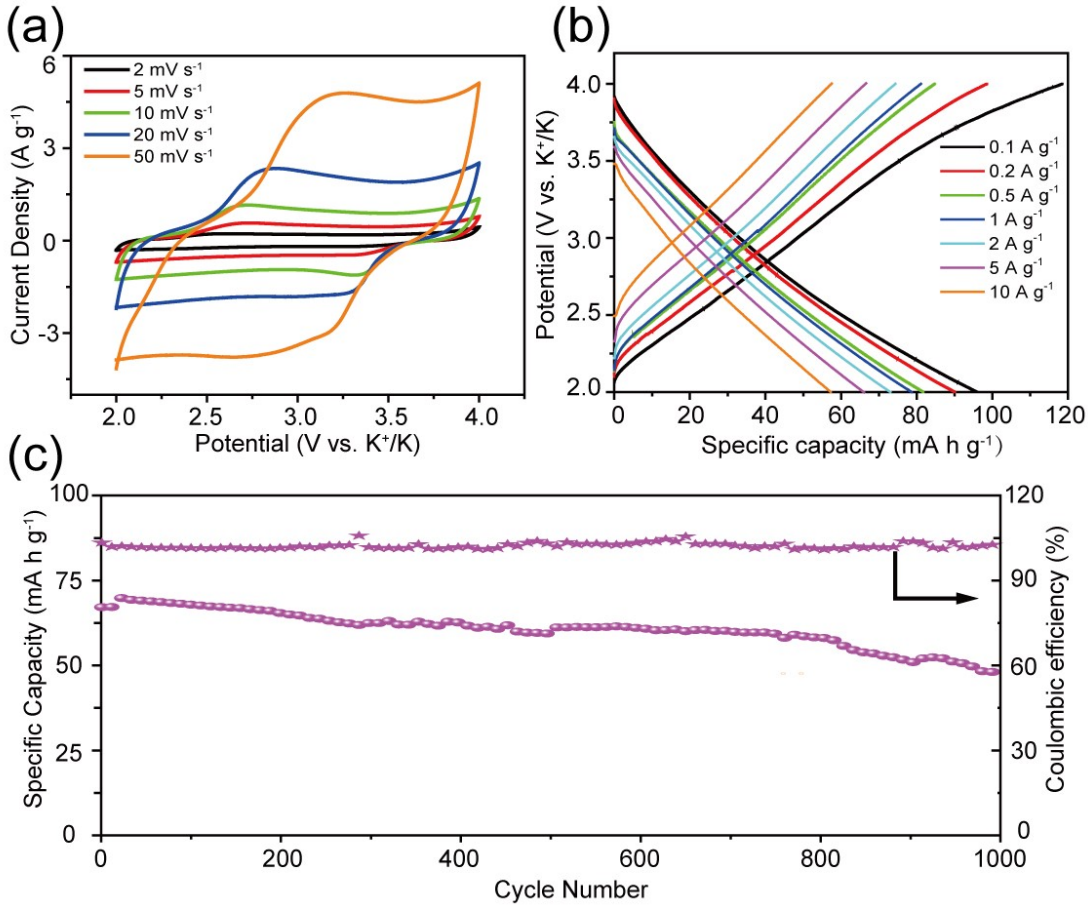

Figure S6. Electrochemical performance of HPC as cathode: (a) CV curves of HPC at various scan rates, (b) GCD curves of HPC at different current density, (c) Cycling performance of at current densities of 2 A g^{-1}

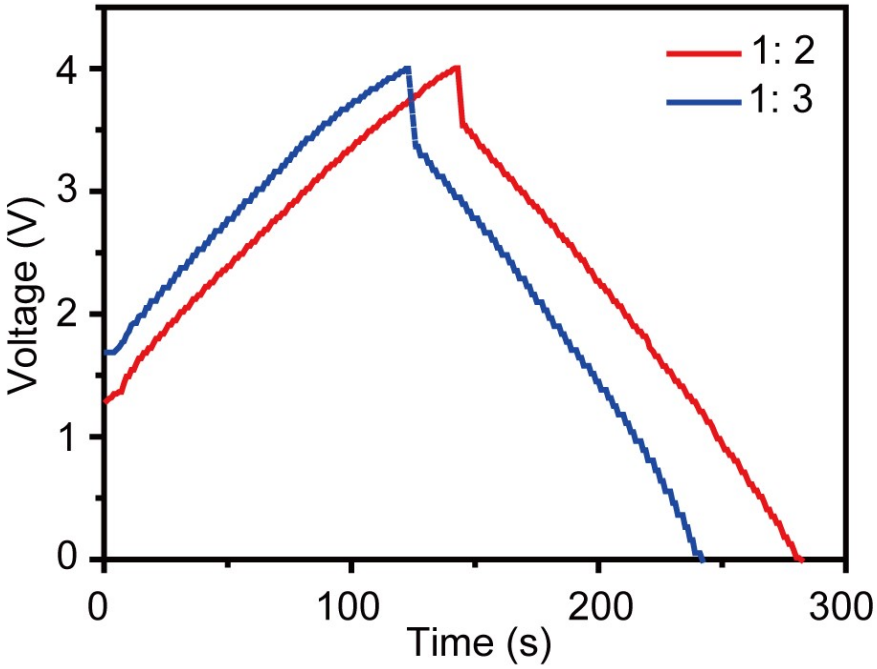

Figure S7. GCD plot of PNC//HPC PIHCs with different mass ratios (1:2 and 1:3) at 1 A g^{-1}

Table S1 Pore structure parameters of all the samples

Sample	[a] S_{BET} (m^2 g^{-1})	[b] V_{total} (cm^3 g^{-1})	[c] $V_{micro\leqslant 0.8nm}$ (cm^3 g^{-1})	[d] V_{micro} (cm^3 g^{-1})	[e] V_{meso} (cm^3 g^{-1})	[f] V_{macro} (cm^3 g^{-1})
NC	301	0.259	0.007	0.051	0.059	0.149
PNC	114	0.177	0.033	0.044	0.047	0.086

a. The specific surface area obtained by BET; b. Total pore volume obtained by DFT; c. Micropore (pore diameter < 0.8 nm) volume calculated by DFT;d. Micropore (pore diameter < 2nm) volume calculated by DFT; e. Mesopore (2 nm≤ pore diameter ≤50 nm) volume calculated by DFT; f. Macropore (50 nm< pore diameter) volume calculated by DFT.

Table S2 Elementary composition evaluated from elemental analysis and relative contents of functional groups in N 1s and C 1s peaks from XPS spectra of different samples

Samples	C	N	O	P	N-6	N-5	N-Q
	(at. %)	(at. %)	(at. %)	(at. %)	(%)	(%)	(%)
NC	87.81	7.5	4.69	--	34.0	46.4	19.6
PNC	83.02	6.37	9.34	1.27	29.7	56.1	14.2

Table S3 Potassium storage performance of PNC compared with previously reported materials

Materials	High rate capability	Cycling performance	Ref.
Hard–soft composite carbon	230 mAh g^{-1} at 140 mA g^{-1} 167 mAh g^{-1} at 1.4 A g^{-1}	200 mAh g^{-1} after 200 cycles at 280 mA g^{-1}	[1]
N-doped hierarchically porous carbon	287.5 mAh g^{-1} at 50 mA g^{-1} 193.1 mAh g^{-1} at 0.5 mA g^{-1}	121 mAh g^{-1} after 1000 cycles at 500 mA g^{-1}	[2]
Graphitic carbon nanocage	221 mAh g^{-1} at 27.9 mA g^{-1} 175 mAh g^{-1} at 9.765 A g^{-1}	195 mAh g^{-1} after 100 cycles at 56 mA g^{-1}	[3]
N/O dual-doped carbon network	464.9 mAh g^{-1} at 50 mA g^{-1}, 175 mAh g^{-1} at 5.0 A g^{-1},	160 mAh g^{-1} after 1000 cycles at 1000 mA g^{-1}	[4]
Hierarchically Porous N-Doped Carbon Fibers	230 mAh g^{-1} at 50 mA g^{-1}	135 mAh g^{-1} after 200 cycles at 500 mA g^{-1}	[5]
Nitrogen-doped hollow carbon nanospheres	326 mAh g^{-1} at 50 mA g^{-1}, 141 mAh g^{-1} at 2 A g^{-1}	154 mAh g^{-1} after 2500 cycles at 1000 mA g^{-1}	[6]
Nitrogen-Doped Hierarchical Porous Carbon	292 mAh g^{-1} at 100 mA g^{-1}, 94 mAh g^{-1} at 10.0 A g^{-1}	157 mA g^{-1} after 12000 cycles at 2000 mA g^{-1}	[7]
PNC	310 mAh g^{-1} at 25 mA g^{-1}, 149 mAh g^{-1} at 5 A g^{-1}	181 mAh g^{-1} after 1000 cycles at 1A g^{-1}	This work

Table S4 Pore structure parameter of HPC

Sample	[a]S_{BET} ($m^2\ g^{-1}$)	[b]S_{micro} ($m^2\ g^{-1}$)	[c]$S_{micro\geq0.8\ nm}$ ($m^2\ g^{-1}$)	[d]S_{meso} ($m^2\ g^{-1}$)	[e]V_{total} ($cm^3\ g^{-1}$)	[f]V_{micro} ($cm^3\ g^{-1}$)	[g]V_{meso} ($cm^3\ g^{-1}$)
HPC	3208	1433	760	699	1.80	0.66	1.10

Table S5 Surface element datum evaluated by XPS of HPC

Sample	C	N	O	O-I	O-II	O-III
	(at.%)	(at.%)	(at.%)	(%)	(%)	(%)
HPC	89.93	1.10	7.86	22.04	59.64	18.34

$i = av^b$ equation S1

$\log(i) = b\log(v) + \log(a)$ equation S2

When b is 0.5, the reaction process is controlled by diffusion (battery behavior). When b is equal to 1, the reaction is controlled by capacitance (capacitive behavior). When b is between 0.5 and 1, the reaction process shows both battery behavior and capacitive behavior [8].

In order to further explore the contribution rate of capacitive behavior to the whole potassium storage behavior, the equation S1 was transformed into [8]：

$i = k_1v + k_2v^{1/2}$ equation S3

where k_1v and $k_2v^{1/2}$ represent capacitance of capacitive behavior contribution and capacity of battery behavior contribution, respectively.

We finally compared the diffusion process of potassium ions in NC and PNC samples by galvanostatic intermittent titration technique (GITT). According to Fick's second law, the diffusion coefficient of electrode materials can be used as follows [9]:

$$D = \frac{4}{\pi\tau}\left(\frac{m_B V_M}{M_B S}\right)^2\left(\frac{\Delta E_S}{\Delta E_\tau}\right)^2$$ equation S4

$$\rho = \frac{1}{V_{total} + \frac{1}{\rho_{carbon}}}$$ equation S5

where τ represents the pulse time (s); m_B is the mass of active material (g); s is geometry area of the electrode; the potential difference (v) caused before and after the current pulse; ΔE_S is the quasi-thermodynamic equilibrium potential difference between before and after the current pulse; ΔE_τ is the potential difference during the current pulse; V_M is the molar volume; M_B is the molar mass of carbon, and the value of the M_B/V_M can be obtained from the density of the sample. In this experiment, the constant current density is 100 mA g^{-1}; discharge pulse time τ is 0.5 h, and relaxation time is 2 h.

REFERENCES

[1] Z. Jian, S. Hwang, Z. Li, A.S. Hernandez, X. Wang, Z. Xing, D. Su, X. Ji, Hard–Soft Composite Carbon as a Long-Cycling and High-Rate Anode for Potassium-Ion Batteries, Adv. Funct. Mater. 27 (2017) 1700324

[2] X. Qi, K. Huang, X. Wu, W. Zhao, H. Wang, Q. Zhuang, Z. Ju, Novel fabrication of N-doped hierarchically porous carbon with exceptional potassium storage properties, Carbon 131 (2018) 79-85

[3] B. Cao, Q. Zhang, H. Liu, B. Xu, S. Zhang, T. Zhou, J. Mao, W.K. Pang, Z. Guo, A. Li, Graphitic Carbon Nanocage as a Stable and High Power Anode for Potassium-Ion Batteries, Adv. Energy Mater. (2018) 1801149.

[4] Ruan J, Zhao Y, Luo S, et al. Fast and stable potassium-ion storage achieved by in situ molecular self-assembling N/O dual-doped carbon network[J]. Energy

Storage Materials 23 (2019) 46-54.

[5] Zhang M, Shoaib M, Fei H, et al. Hierarchically Porous N-Doped Carbon Fibers as a Free-Standing Anode for High-Capacity Potassium-Based Dual-Ion Battery[J]. Adv. Energy Mater. 9 (2019) 1901663.

[6] Ruan J, Wu X, Wang Y, et al. Nitrogen-doped hollow carbon nanospheres towards the application of potassium ion storage[J]. J. Mater. Chem. A 7 (2019) 19305-19315.

[7] Zhou X, Chen L, Zhang W, et al. Three-Dimensional Ordered Macroporous Metal–Organic Framework Single Crystal-Derived Nitrogen-Doped Hierarchical Porous Carbon for High-Performance Potassium-Ion Batteries[J]. Nano Lett. 19 (2019) 4965-4973.

[8] Wang J, Polleux J, Lim J, et al. Pseudocapacitive contributions to electrochemical energy storage in TiO_2 (anatase) nanoparticles[J]. J. Phys. Chem. C 111 (2007) 14925-14931.

[9] Shen Z, Cao L, Rahn C D, et al. Least squares galvanostatic intermittent titration technique (LS-GITT) for accurate solid phase diffusivity measurement[J]. J. Electrochem. Soc. 160 (2013) A1842.